The effect of alginates, fucans and phenolic substances from the brown seaweed *Padina gymnospora* in calcium carbonate mineralization *in vitro*

L.T. Salgado [a], G.M. Amado Filho [a], M.S. Fernandez [b], J.L. Arias [b], M. Farina [c,*]

[a] *Diretoria de Pesquisas, Instituto de Pesquisas Jardim Botânico do Rio de Janeiro, Rio de Janeiro 22460-030, Brasil*
[b] *Department of Animal Biology, Faculty of Veterinary and Animal Sciences, and CIMAT, University of Chile, Santiago, Chile*
[c] *Laboratório de Biomineralização, Instituto de Ciências Biomédicas, Universidade Federal do Rio de Janeiro, Rio de Janeiro 21941-902, Brasil*

ABSTRACT

The mineralization of calcium carbonate ($CaCO_3$) in the brown seaweed *Padina gymnospora* is a biologically induced process and is restricted to the cell wall surface. It has been suggested that the $CaCO_3$ crystallization that occurs over the thallus cell wall surface is induced by changes in the surface pH caused by a local efflux of OH^-, Ca^{++} and HCO_3^- ions. However, no studies on the roles of the *P. gymnospora* cell wall components in this mineralization process had been performed. Therefore, we evaluated the influence of a subset of *P. gymnospora* cell wall molecules on $CaCO_3$ crystallization *in vitro*. The molecules tested were the anionic polysaccharides alginates and fucans (with potential nucleation activity) and phenolic substances (secondary metabolites with amphipathic property). The crystallization assays were performed using polystyrene microbridges as the crystallization apparatus. Crystals formed in the microbridges were analyzed using scanning electron microscopy. Interestingly, the results confirmed that the phenolic substances have the specific capability of changing the morphology of calcite crystals grown *in vitro* by inducing an elongated morphology in the direction of the *c*-axis. This morphology is similar to that induced by molecules that attach to {*h k* 0}-crystal planes. It was also shown that the alginates and the fucans do not specifically modulate the morphology of the growing crystals. In fact, these crystals exhibited a rounded shape due to the slower growth rates of several new crystal planes that appeared in the place of the original corners and edges.

© 2011 Elsevier B.V. All rights reserved.

1. Introduction

Calcification in algae can be grouped into three different types [1]: the first is the intracellular calcification that occurs in unicellular algae assigned to the family Coccolithophoraceae; the second is the calcification of the cell walls that occurs in Corallinaceae algae; the third comprises the intercellular calcification (observed in *Halimeda discoidea*) [1–4] and the extracellular calcification observed in the brown alga *Padina gymnospora*, in which crystallites of the calcium carbonate polymorph aragonite are seen [1,2].

Classically, the crystallization process is a two-step phenomenon consisting of crystal nucleation and crystal growth [5]. The main chemical conditions that affect crystallization are the pH and the Ca^{++} and CO_2 availability. These conditions can be modified by the mineralizing organism through the use of proton-pumps (to modify the pH), Ca^{++}ATPase pumps (to control the

concentration of the Ca^{++} ions) and carbonic anhydrase enzymes (to control the CO_2 concentration close to the calcification regions) [1,6–9]. Moreover, the crystallization process depends on the presence of nucleation cores, e.g., anionic molecules, including selected peptides and polysaccharides [1].

In brown algae, two main polysaccharides, the alginates and the sulfated fucans, have been implicated in the mineralization process [10]. It is known that calcium binding promotes alginate self-assembly and, consequently, the formation of the "egg-box" structure [10]. Recently, it was shown that the alginates may act as organic templates for an electrodeposited calcium carbonate coating [11]. The sulfated fucans are also capable of trapping cations, specifically cadmium and zinc [12]. These two polysaccharides are abundant in cell walls. Interestingly, they are preferentially distributed along the outer layers of the cortical cell walls [1,10,12,13].

This data raise the question whether calcification is related to the preferential distribution of these polysaccharides along the outer layers of the cortical cell walls. If this were the case, then the entire thallus surface would be expected to be calcified. However, it has been reported that *P. gymnospora* displays an

* Corresponding author. Tel.: +55 21 25626393; fax: +55 21 25626480.
  E-mail address: mfarina@anato.ufrj.br (M. Farina).

alternating pattern of calcified and non-calcified areas [14]. Therefore, other possible molecular activities influencing the mineralization process must be considered.

Recently, the phenolic substances were confirmed as novel constituents of brown algae cell walls [15,16]. These substances are secondary metabolites found within the physodes and also in cell walls strongly linked with the alginates [13,15,16]. The phenolic substances found in *P. gymnospora* are amphipathic (due to the presence of a fatty acid chain), form polymeric chains and, when linked to the alginates, form high molecular weight complexes [16].

To our knowledge, no studies on a possible role of the phenolic substances in the calcification process have been performed until now. Interestingly, a recent report showed that different fatty acids tested in crystallization assays caused different patterns of $CaCO_3$ mineralization [17]. By analogy, the activity of the phenolic substances could be similar to that of the fatty acids and therefore must be investigated. In addition to testing the effects of the phenolic substances on the calcification process, the activity of the alginates and the sulfated fucans must be tested for comparison. Consequently, the aim of our work was to determine the effect of the phenolic substances and the anionic polysaccharides (the alginates and the fucans) extracted from the brown seaweed *P. gymnospora* on $CaCO_3$ crystallization *in vitro*.

2. Experimental details

2.1. Algae collection

Samples of adult *P. gymnospora* 5 cm in length were collected in the upper region of the sub-tidal zone in Sepetiba Bay, located in the state of Rio de Janeiro, Brazil ($22°57'05''S$ and $43°54'28''W$). The algae were taken to the laboratory in a dark isotherm chamber containing seawater. A sample (10 g) of these algae was washed in distilled H_2O and dried at 60 °C for the subsequent extraction of the polysaccharides and the phenolic substances.

2.2. Scanning electron microscopy of $CaCO_3$ crystals naturally grown on the P. gymnospora thallus surface

Fresh fragments (2.0 mm) of the *P. gymnospora* thallus were air-dried and mounted on appropriate stubs, gold-sputtered (Sputter coater Bal-Tec SCD 050) and observed using a Zeiss EVO 40 scanning electron microscope operated at 15 kV.

2.3. Isolation of the polysaccharides and phenolic substances

Polysaccharide extraction and purification were performed according to Salgado et al. [15,16]. Briefly, the polysaccharide fraction was extracted from dry algae by papain digestion for 24 h at 60 °C. The obtained polysaccharide fraction was dialyzed against 10% EDTA and against distilled H_2O (72 h each). After lyophilization, the sample was submitted to anion-exchange chromatography using a Mono-Q column HR 5/5 (Amersham Pharmacia Biotech). The column, linked to an FPLC system (Amersham Pharmacia Biotech) was equilibrated in 20 mM Tris–HCl (pH 8.0) 5 mM EDTA. The polysaccharides were eluted with a linear gradient of NaCl (up to 3 M) at a flow rate of 0.5 mL/min. The presence of uronic acid, the fucans and the total polysaccharides were quantified using DMB, carbozole and phenol-H_2SO_4 reactions, respectively. The concentration of NaCl was determined by measuring conductivity. The obtained fractions were dialyzed against distilled H_2O and lyophilized. After acid hydrolysis, the monosaccharide composition was estimated by paper chromatography in 1-butanol/pyridine/water (3:2:1, v/v) during 48 h.

As previously reported [16], the phenolic substances synthesized by *P. gymnospora* are primarily composed of 2-[1'-*Oxohexadecyl*]-1,3,5-trihydroxybenzene (Fig. 2) and have a molecular weight close to 10 kDa. This structure is composed of an aromatic ring attached to three hydroxyls (1-3-5) and a carbonic chain (16 C) [16]. The extraction of soluble phenolic substances was performed according to Salgado et al. [15,16]. Dried alga (25 g) was maintained in a 75% acetone aqueous solution (1 L) for 48 h. Thereafter, the acetone was evaporated, and the pellet was dissolved in distilled H_2O, centrifuged again, and the soluble fraction was lyophilized. The extracted phenolic substances were diluted in distilled H_2O and partially purified using a C-18 column (Sep-Pak C-18 Cartridge, Water Associates, Millipore™, Billerica, MA, USA). The column was activated with ethanol and washed with distilled H_2O. Elution of the phenolic substances from the column was performed with a linear gradient of ethanol. The obtained fractions were evaporated and the residue dissolved in distilled H_2O and lyophilized. Fractions with isolated phenolic substances were purified using size exclusion chromatography (SEC) and a Superose 6 column (Amersham Pharmacia Biotech, Buckinghamshire, United Kingdom) linked to an HPLC system from Shimadzu (Tokyo-Japan). The column was equilibrated with 100 mM sodium acetate buffer (pH 6.3) 20 mM EDTA and 250 mM NaCl. The flow rate of the column was 15 mL/h. The fractions were monitored by absorbance at 210 nm. The molecular weight standards used to mark V_o and V_t were dextran blue and glycine, respectively. During these procedures, we were careful to protect the samples from degradation by radiation.

2.4. $CaCO_3$ crystallization assays

The crystallization assays were performed in accordance with Fernandez et al. [18] using polystyrene microbridges (Hampton Res.) as the crystallization apparatus. The microbridges were placed in a homemade closed chamber built with an 85 mm plastic Petri dish with a central hole in its bottom (15 mm diameter). The free surface of the bottom of the Petri dish was divided into eight regions by eight radial lines to assure an equidistant distribution of microbridges from the central region. A plastic cylindrical vessel (15 mm diameter/30 mm height) was glued to the contour of the central hole, making a T-shaped apparatus when observed from its side. The microbridges were filled with 35 µl of 200 mM $CaCl_2$ in 200 mM TRIS buffer (pH 8.5). The bottom of the cylindrical vessel contained 3 ml of 25 mM ammonium carbonate (NH_4HCO_3). The experiments were run at 20 °C for 36 h. The theoretical basis for this method of crystallization is based on the diffusion of CO_2 into $CaCl_2$ solutions to cause $CaCO_3$ to precipitate onto the bottom surface of the microbridges. A control assay, which did not contain added polysaccharides or phenolic substances, confirmed that the experimental conditions were appropriate when mainly rhombohedral calcite crystals were observed. The influence of the polysaccharides and the phenolic compounds on crystallization was evaluated separately by diluting each compound in $CaCl_2$ solutions in three different concentrations (20, 10 and 5 µg/ml). The pH values (8.5) of these solutions were not modified by the addition of the polysaccharides and phenolic compounds. After each experimental assay, microbridges were carefully washed with distilled water, air-dried, mounted on aluminum stubs, gold-sputtered (BAL-TEC SCD 050) and observed using a Jeol 5310 scanning electron microscope operated at 20 kV.

2.5. Electron diffraction analysis of $CaCO_3$ mineralized in vitro

Calcium carbonate crystals from the mineralization assay in the presence of 20 µg/mL of phenolic substances were ground to

powder in a dry condition inside the same microbridges where the mineralization occurred. The powdered material was mixed with few microliters of distilled water and a drop (~3 μL) containing the crystals was deposited on a formvar coated 300 mesh copper grid, and excess water removed by filter paper and air dried. Bright field images and electron diffraction patterns from a selected area were obtained with a Zeiss 900 transmission electron microscope operated at 80 kV equipped with a CCD camera (MegaviewIII Soft Imaging System—Olympus).

3. Results

The calcium carbonate crystals found in *P. gymnospora* were mainly observed on the ventral thallus surface distributed in alternating bands parallel to the apical margin of the alga (Fig. 1a,b). A detailed observation revealed that mineralization was absent in some thallus regions (Fig. 1c), while in other areas the mineralization varied from discrete (Fig. 1d) to very intense (Fig. 1f). When mineralization was discrete, the organization of the calcium carbonate crystals, as well as their needle-like morphology, could be determined. The major axis of the crystals was oriented parallel to the cell wall surface (Fig. 1e). The crystal deposits were primarily observed on wall regions between the cortical cells, just over the anticlinal walls (Fig. 1e). In addition to

exhibiting an elongated shape, the $CaCO_3$ crystals showed a smooth variation in thickness and structures similar to rigid sheets where twin-like crystal arrangements were formed (Fig. 2).

Two main polysaccharide fractions were obtained from *P. gymnospora*: the fucans and the alginates. Paper chromatography
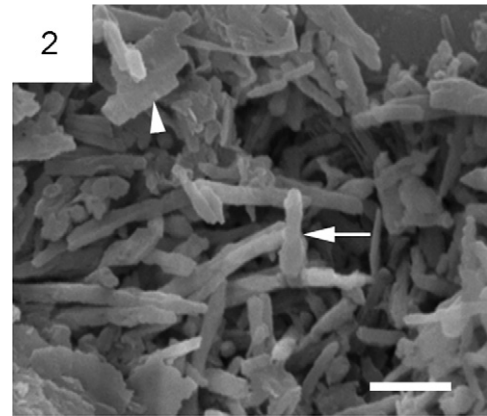

Fig. 2. SEM of calcium carbonate crystals growing over the thallus surface of *P. gymnospora*. Crystals present an elongated shape with smooth variations in thickness (arrow); structures similar to rigid plates resembling a twin-like crystal arrangement are also observed (arrowhead). Bar=1 μm.
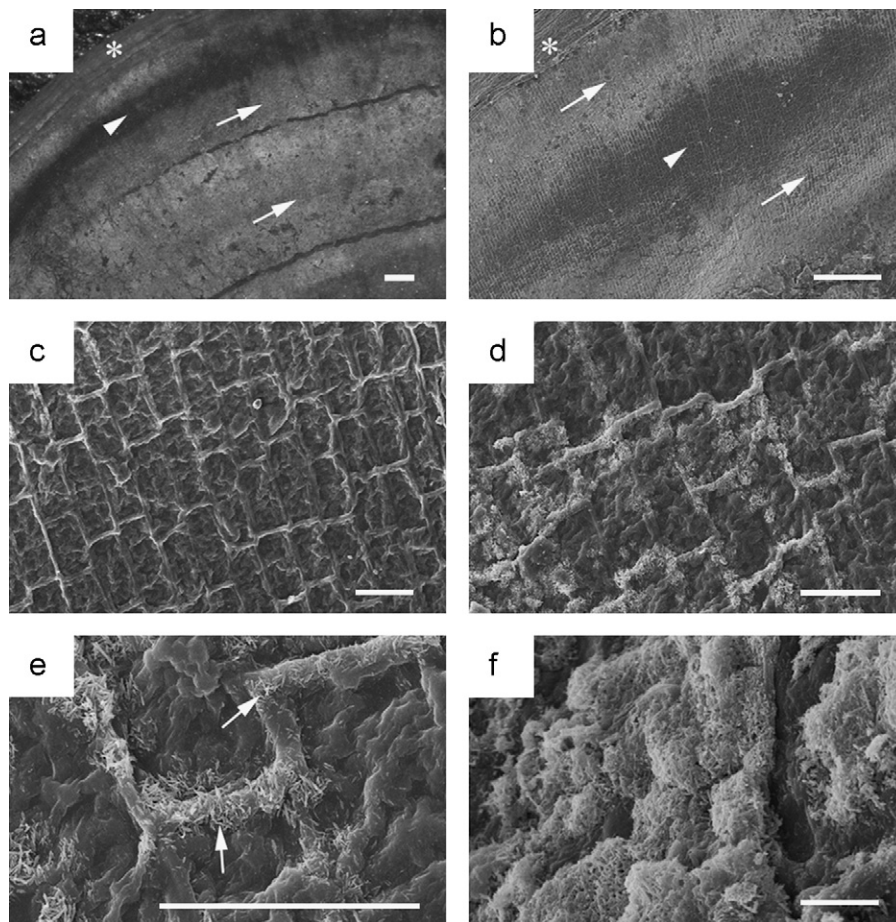

Fig. 1. Optical stereomicroscopy and scanning electron microscopy (SEM) of a thallus surface of *P. gymnospora*. (a) An image of the *P. gymnospora* thallus surface observed by optical steromicroscopy, where many calcified (arrows) and non-calcified regions (arrowhead) can be distinguished, *—apical margin (bar=350 μm); (b) low-magnification scanning electron micrograph (SEM) of the region of the *P. gymnospora* thallus, where detail of the alternating mineralized (arrows) and non-mineralized bands (arrowhead) can be observed, *—apical margin (bar=350 μm); (c) SEM of the ventral region of the thallus showing the cortical cells and few mineralized regions; (d) SEM of the ventral region of the thallus showing the cortical cells and many mineralized regions; (e) SEM image of the ventral surface showing that calcium carbonate crystals are mainly distributed along the walls outlining the cortical cells (arrows); (f) ventral view of the thallus surface showing a highly mineralized area. Bars for c, d, e and f=30 μm.

revealed that the fucans (fraction 1) were primarily composed of fucose residues and low concentrations of galactose and glucose residues, while the alginates (fraction 2) were composed of an undetermined mixture of uronic acid residues. The isolated phenolic substances were identified as the same type that has been described in previous works, as they were composed of 2-[1′-Oxo-hexandecyl]-1,3,5-trihydroxybenzene [15,16].

In the crystallization assays, rhombohedral calcite crystals were formed in the control experiment as expected (Fig. 3). The morphology of the calcium carbonate crystals from the micro-bridges containing the alginates and the sulfated fucans was different from but still very similar to that obtained in the control assay. The crystals exhibited a rounded shape with several new
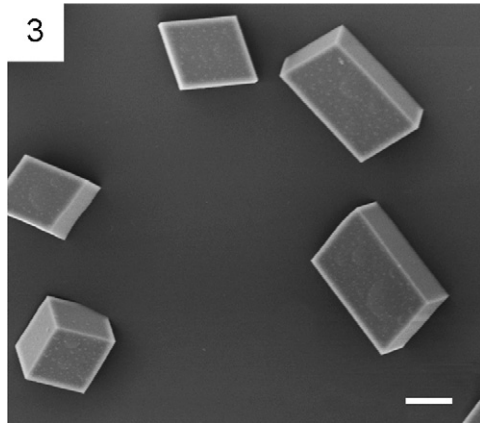

Fig. 3. SEM of calcite crystals grown *in vitro*. Representative image of typical rhombohedral calcite crystals from the control assay. Bar=8 μm.

faces replacing the original corners and edges between the {1 0 4} faces that would commonly be observed in the rhombohedral morphology (Fig. 4a–d and Fig. 5a–d). The modification to the calcite rhombohedral morphology was more evident in crystals grown in higher concentrations (20 μg/ml) of the alginates and the fucans (Fig. 4a,b and Fig. 5a,b). On the other hand, the addition of the phenolic substances to the $CaCl_2$ solution caused a specific modification to the morphology of the growing crystals. Some faces of the calcite crystals were specifically inhibited, and the appearance of the crystal structure changed (Fig. 6a–g). Complex structures elongated along the *c*-axis were seen (Fig. 6a–c). However, when the concentrations of the phenolic substances were lowered (10 and 5 μg/ml), the morphology of the calcite crystals appeared to be similar to that observed for crystals grown in the presence of the alginates and the fucans (Fig. 6d–g).

4. Discussion

One of the most accepted hypotheses on the mineralization process in *P. gymnospora* is that the $CaCO_3$ crystallization is induced by changes in the pH of the cell wall surface caused by the local efflux of OH^- ions [1]. Based on this hypothesis, it would be reasonable to expect a uniform calcification over the entire thallus surface or at least concentrated calcification just over the cell compartments, where the flux of ions is more intense. In contrast, the needle-like crystals were distributed only over the walls outlining the cortical cells and not over the cell compartments (Fig. 1c,d). Thus, other factors may influence the biomineralization process on specific regions of the thallus surface, such as anti-calcification molecular activity or a higher rate of $CaCO_3$ nucleation activity. Moreover, at thallus regions where the crystallization occurs, the vicinity of the plasmalemma may allow
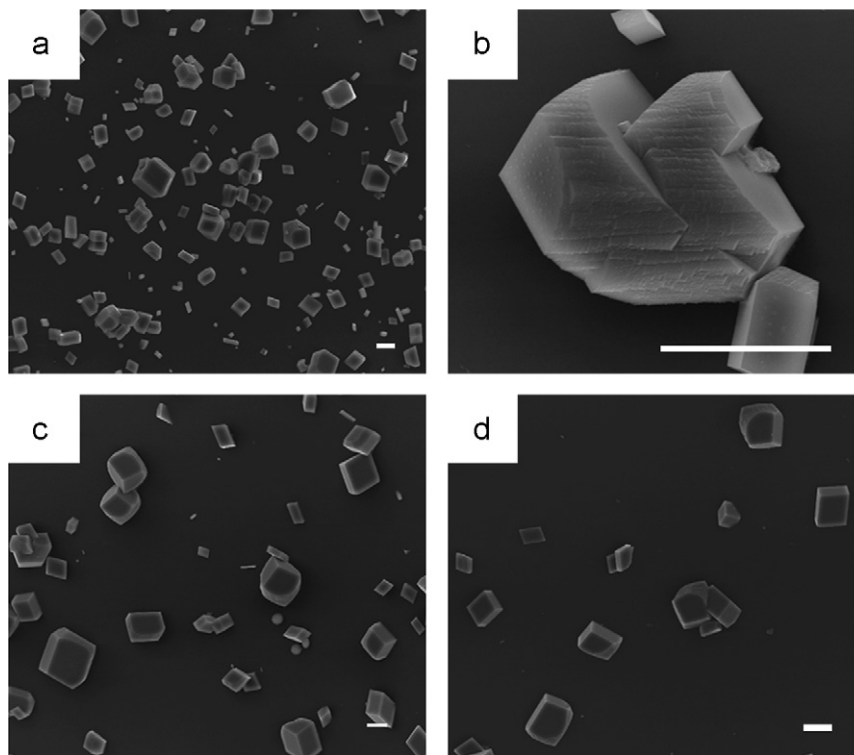

Fig. 4. SEM images of calcite crystals grown in the presence of alginates isolated from *P. gymnospora* brown seaweed. (a) Calcite crystals grown in an alginate concentration of 20 μg/mL. Note the rounded appearance of the crystals; (b) detail of a calcite crystal grown in an alginate concentration of 20 μg/mL revealing several new crystal planes that appear in the place of the original corners and edges between the {1 0 4} faces; (c and d) calcite crystals grown in alginate concentrations of 10 and 5 μg/mL, respectively. The alterations in calcite crystal morphology decreased simultaneously with the reduction of the alginate concentration. Bars=10 μm.
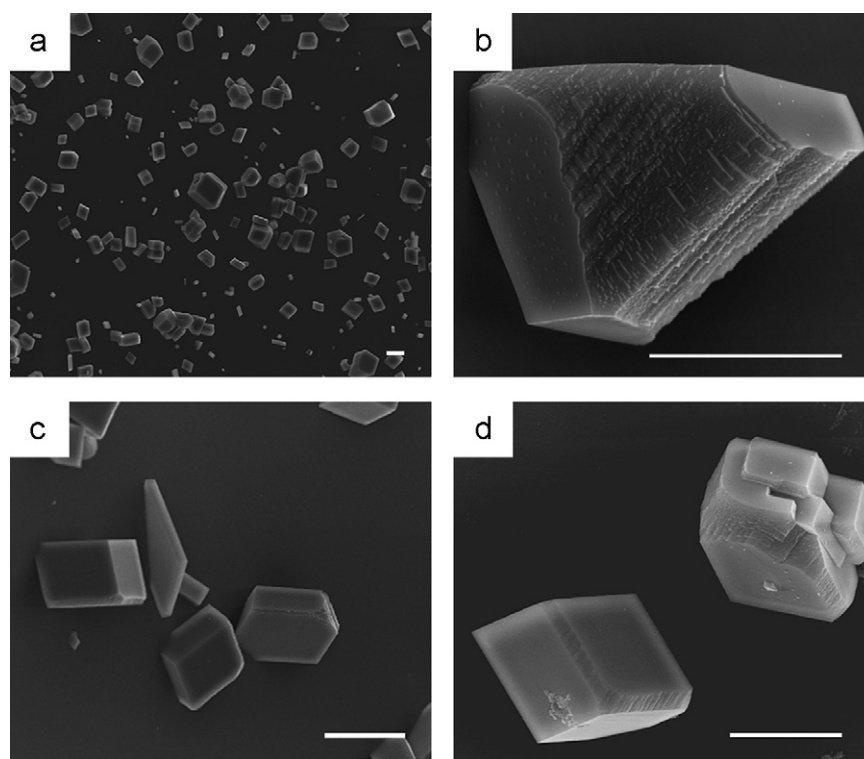
Fig. 5. SEM images of calcite crystals grown in the presence of fucans isolated from *P. gymnospora* brown seaweed. Crystals exhibit similar aspects to the crystals grown in the alginate-containing solutions. (a) Calcite crystals grown in a fucans concentration of 20 µg/mL. Note the rounded appearance of the crystals; (b) detail of a calcite crystal grown in a fucans concentration of 20 µg/mL revealing several new crystal planes that appear in the place of the original corners and edges; (c and d) Calcite crystals grown in fucans concentrations of 10 and 5 µg/mL, respectively. The alterations in the calcite crystal morphology decreased simultaneously with the reduction of the fucans concentration. Bars = 12 µm.

exocytosed substances with anti-calcification molecular activity to reach the extracellular space more easily by passing through their thin cell walls. In addition, it has been shown that the cell wall regions delimiting cortical cells may exhibit higher amounts of polyanionic polysaccharides [12], which could increase $CaCO_3$ nucleation.

Among the studies on the main constituents of brown algal cell walls, many have confirmed the polyanionic polysaccharides and phenolic substances as natural cell wall compounds, which arise from an exocytic pathway [10,13,16]. Until now, only the role of alginic acid in the nucleation of $CaCO_3$ crystals *in vitro* had been tested [11]. Pavez et al. [11] revealed that alginic acids can act as template for calcite crystal growth. However, the capability of this molecule and other brown algal cell wall molecules to influence the growth of crystals was not tested.

In our assays, the two isolated polysaccharides, the alginates and the fucans, only induced unspecific morphological modifications to growing calcite crystals, which were described as "rounded calcite crystals". When higher concentrations of polysaccharides were tested, these changes were more pronounced. Collectively, these results provide evidence that the polysaccharides have a stochastic effect on crystal growth, once that these data are analogous to those obtained by Shen et al. [19], which tested the effects of collagen on the morphology of calcite crystals grown *in vitro*. Compared with the collagen activity, the effect of the alginates and the fucans on crystal morphology was similar, as they inhibited growth of some specific crystal planes due to competition with inorganic ions. It was proposed that the random inhibition of the formation of the calcite crystal planes occurs because collagen is non-uniformly incorporated into the calcite crystal planes [19]. These slower-growing planes are numerous and dominate the calcite morphology. Therefore, crystals exhibit a rounded shape. Thus, the alginates and the fucans likely

decrease the velocities of crystal growth in the corners and edges where potential planes are located, thereby causing the observed rounded calcite morphology. In addition, it has been shown that the crystal rounding and the occurrence of the calcium carbonate polymorphism depend on the concentration of the alginates [20].

The observed modifications to the morphology of calcite crystals grown in the presence of solutions containing phenolic substances revealed a specific activity of these molecules. A possible explanation for this activity is the presence of a fatty acid chain attached to the phloroglucinol unit of the phenol molecule. Recently, it was shown that variations in the length of the carbon chain of fatty acids resulted in different morphologies of calcite crystals grown *in vitro* [17]. In this study, the chain length was considered one of the main factors determining the velocity of crystal growth and crystal polymorphism. The mineralization of aragonite was observed when crystallization was performed in the presence of palmitic acid (PA), which contains a chain length of 16 carbons [17], like the 2-[1′-*Oxo-hexandecyl*]-1,3,5-trihydroxybenzene phenolic substance found in *P. gymnospora*.

The crystals grown in solutions containing the phenolic substances strikingly resembled the calcite crystals grown in the presence of calcium binding protein 1 (CBP1) [21]. CBP1 is a constructed peptide that, when tested *in vitro*, also generated complex structures elongated along the [0 0 1] direction (*c*-axis) with rhombohedral {1 0 4} faces [21]. The main explanation attributed to these results was the structural property of the peptide (89% in α-helix conformation), which may adhere to specific crystal faces, thus inhibiting their growth by competing with carbonate groups [21]. CBP1 displays activity that resembles analogs of antifreeze polypeptides (AFP), because it was only at lower temperatures that the elongation of the crystals and the specific crystal planes inhibition could be observed [21]. Most likely, the amphipathic structure of the phenolic substances, as well as their arrangement in polymeric chains, is related to their
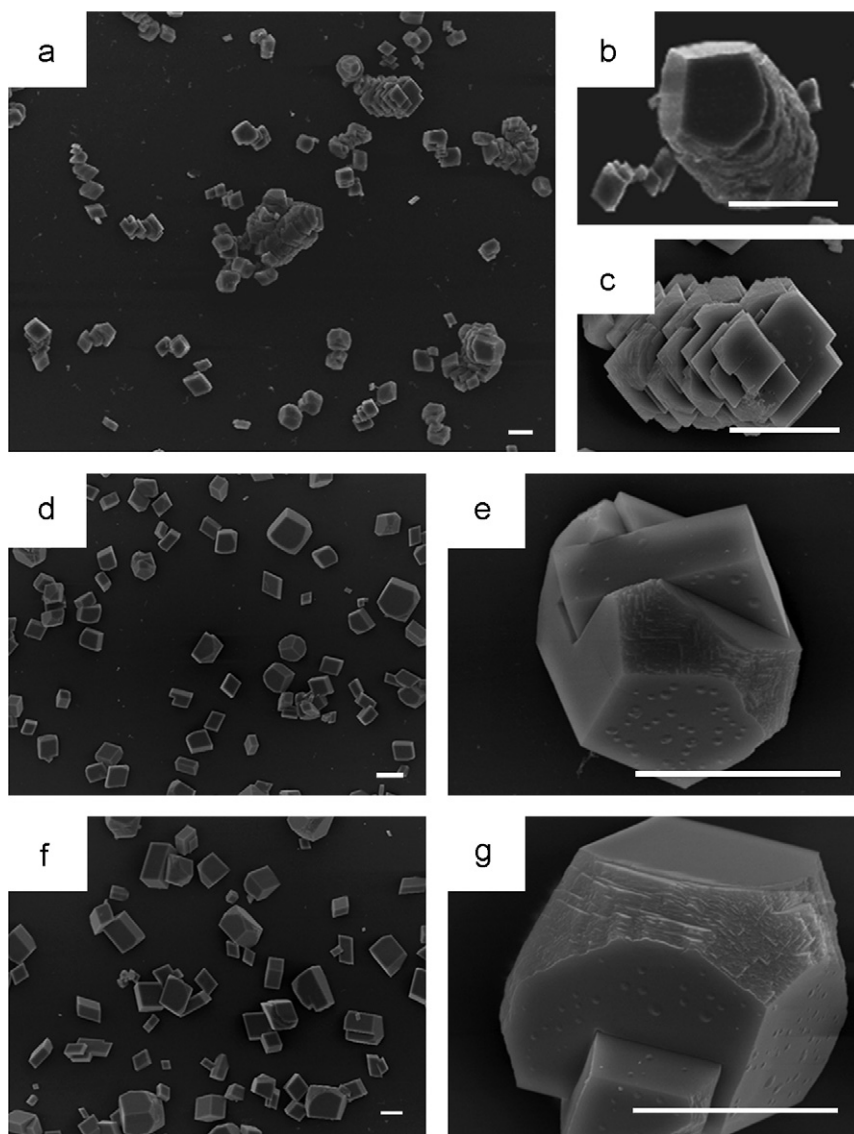
Fig. 6. SEM of calcite crystals grown in the presence of the phenolic substances isolated from *P. gymnospora* brown seaweed. (a) A low magnification view of calcite crystals grown in the phenolic substances at a concentration of 20 µg/mL; (b,c) detailed observation of calcite crystals grown in the phenolic substances at a concentration of 20 µg/mL. The morphology of the crystals appears specifically modified when compared to that of the calcite crystals shown in the control assays (see Fig. 3). Complex crystal structures are elongated in the direction of the *c*-axis similar to that observed for CBP1 [21]. (d–g) Calcite crystals grown in the phenolic substances at concentrations of 10 µg/mL (d,e) and 5 µg/mL (f,g). The alterations to the morphology of the calcite crystals decreased simultaneously with a reduction in the phenolic substances concentration. At these concentrations, crystals are more rounded and less elongated. Bars in all micrographs=10 µm.

effect on calcite crystal growth [15]. Following this cue, we suggest that the hydroxyl or the carbonyl groups of the 2-[1′-Oxo-hexandecyl]-1,3,5-trihydroxybenzene interacts with the Ca^{++} of the crystals.

In conclusion, it was shown that the alginates and the fucans generated calcite crystal morphology exhibiting a rounded shape due to the slower growth rate of crystals in several new crystal planes, which are mainly located in the corners and edges of the original crystal. However, this result does not exclude the possible participation of these polysaccharides in calcium nucleation. We also confirmed that the phenolic substances are capable of specifically changing the morphology of calcite crystals grown *in vitro* by attaching to crystal faces of the type {h k 0}. The presence of elongated calcite and the absence of aragonite in the *in vitro* mineralization assays show that although phenolic substances can influence calcium carbonate crystal morphology, they do not specifically control the polymorph mineralization process.

The analysis by electron diffraction confirmed that crystals grown in the presence of phenolic substances are constituted by calcite (Fig. 7). Thus, other factors may influence the *in vivo* precipitation of aragonite, including, among others, the speed of OH^-, Ca^{++} and HCO_3^- efflux from the cell, the organization pattern of macromolecules in the cell wall and the flux gradients. We suggest that the absence of calcium carbonate in the cell wall matrix of *P. gymnospora* may be caused by the specific activity of the phenolic substances, which are more concentrated in the less mineralized regions of *P. gymnospora*. Perhaps the alternation of mineralized and non-mineralized layers in the thallus surface is a consequence of the different cellular activities throughout the alga life cycle (growth/arrest) that up- or down-regulate the exocytosis of phenolic substances to the cell walls. Finally, the specific activity of the phenolic substances on the growth of calcite crystals could indicate a potential application of this group of molecules in biomimetic studies.
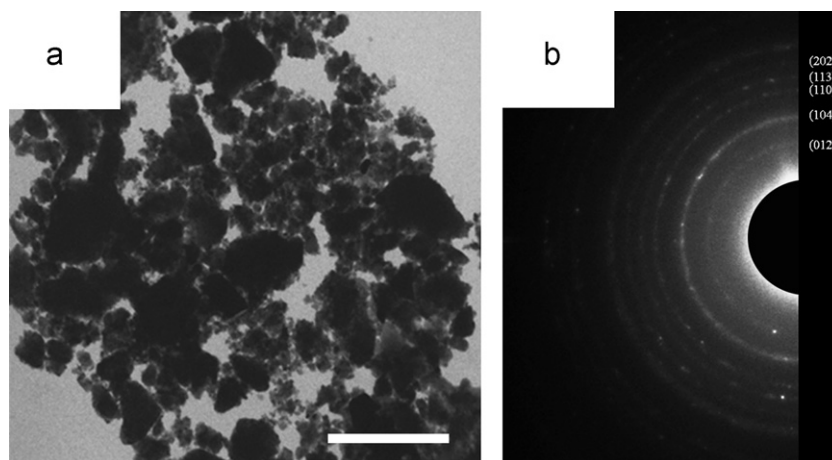
Fig. 7. Transmission electron microscopy (TEM) image and electron diffraction pattern of crystals grown in the presence of the phenolic substances (20μg/mL). (a) Bright field image of a powdered sample deposited on a formvar coated 300 mesh copper grid; (b) electron diffraction pattern of the same area shown in fig. 7a where the diffraction rings analyzed correspond to the calcite lattice planes (0 1 2), (1 0 4), (1 1 0), (1 1 3) and (2 0 2). Bar=0.8 μm.

Acknowledgement

References

[1] M.A. Borowitzka, The morphology and cytology of calcium carbonate deposition by algae, Int. Rev. Cytol. 74 (1982) 127–162.
[2] M.I. Bilan, A.I. Usov, Polysaccharides of calcareous algae and their effect on the calcification process, Russ. J. Bioorg. Chem. 27 (2001) 2–16.
[3] K. Zetsche, Differences in composition of cell wall of stalk and cap by *Acetabulria mediterranea*, Planta 76 (1967) 326–334.
[4] B.S.C. Leadbeater, R. Riding, Biomineralization in Lower Plants and Animals, Oxford University Press, USA, 1986.
[5] S. Weiner, Biomineralization: a structural perspective, J. Struct. Biol. 163 (2008) 229–234.
[6] D. De Beer, A.W.D. Larkum, Photosynthesis and calcification in the calcifying algae *Halimeda discoidea* studied with microsensors, Plant Cell Environ. 24 (2001) 1209–1217.
[7] S. Ray, M. Klenell, K. Choo, M. Pedersén, P. Snoeijs, Carbon acquisition mechanisms in *Chara tomentosa*, Aquat. Bot. 76 (2003) 141–154.
[8] T.A. McConnaughey, R.H. Falk, Calcium-proton exchange during algal calcification, Biol. Bull. 180 (1991) 185–195.
[9] G.D. Price, M.R. Badger, M.E. Bassett, M. Whitecross, Involvement of plasmalemmasomes and carbonic anhydrase in photosynthetic utilization of bicarbonate in *Chara corallina*, Aust. J. Plant Physiol. 12 (1985) 241–256.
[10] B. Kloareg, R.S. Quatrano, Structure of the cell walls of marine algae and ecophysiological functions of the matrix polysaccharides, Oceanogr. Mar. Biol. Annu. Rev. 26 (1988) 259–315.

[11] J. Pavez, J.F. Silva, F. Melo, Effects of alginic acid from marine algae on calcium carbonate electrodeposited coating, J. Cryst. Growth 282 (2005) 438–447.
[12] L.R. de Andrade, M. Farina, G.M. Amado Filho, Role of *Padina gymnospora* (Dictyotales, Phaeophyceae) cell walls in cadmium accumulation, Phycologia 41 (2002) 39–48.
[13] L.T. Salgado, L.R. Andrade, G.M. Amado-Filho, Localization of specific monosaccharides in cells of the brown alga *Padina gymnospora* and the relation to heavy-metal accumulation, Protoplasma 225 (2005) 123–128.
[14] C.A.G. Nassar, L.T. Salgado, Y. Yoneshigue-Valentin, G.M. Amado-Filho, The effect of iron-ore particles on the metal content of the brown alga *Padina gymnospora* (Espirito Santo Bay, Brazil), Environ. Pollut. 123 (2003) 301–305.
[15] L.T. Salgado, R. Tomazetto, L.P. Cinelli, M. Farina, G.M. Amado-Filho, The influence of brown algae alginates on phenolic compounds capability of ultraviolet radiation absorption in vitro, Braz. J. Oceanogr. 55 (2007) 145–154.
[16] L.T. Salgado, L.P. Cinelli, N.B. Viana, R. Tomazetto, P.A.S. Mourão, V.L. Teixeira, M. Farina, G.M. Amado-Filho, A vanadium bromoperoxidase catalyzes the formation of high-molecular-weight complexes between brown algal phenolic substances and alginates, J. Phycol. 45 (2009) 193–202.
[17] E. Loste, E. Diaz-Marti, A. Zarbakhsh, F.C. Meldrum, Study of calcium carbonate precipitation under a series of fatty acid Langmuir monolayers using Brewster Angle Microscopy, Langmuir 19 (2003) 2830–2837.
[18] M.S. Fernandez, K. Passalacqua, J.I. Arias, J.L. Arias, Partial biomimetic reconstitution of avian eggshell formation, J. Struct. Biol. 148 (2004) 1–10.
[19] F.H. Shen, Q.L. Feng, C.M. Wang, The modulation of collagen on crystal morphology of calcium carbonate, J. Cryst. Growth 242 (2002) 239–244.
[20] M. Diaz-Dosque, P. Aranda, M. Darder, J. Retuert, M. Yazdani-Pedram, J.L. Arias, E. Ruiz-Hitzky, Use of biopolymers as oriented supports for the stabilization of different polymorphs of biomineralized calcium carbonate with complex shape, J. Cryst. Growth 310 (2008) 5331–5340.
[21] D.B. de Oliveira, R.A. Laursen, Control of calcite crystal morphology by a peptide designed to bind to a specific surface, J. Am. Chem. Soc. 119 (1997) 10627–10631.